

*J. Electroanal. Chem.*, 262 (1989) 83–95  
Elsevier Sequoia S.A., Lausanne – Printed in The Netherlands

## **Dc anodic stripping voltammetry at mercury thin film electrodes: the shape and position of the stripping peaks at hydrodynamic electrodes**

**Christopher M.A. Brett and Ana Maria C.F. Oliveira Brett**

*Departamento de Química, Universidade de Coimbra, 3049 Coimbra (Portugal)*

(Received 25 August 1988; in revised form 24 November 1988)

### **ABSTRACT**

The shape and position of the stripping peaks in dc (linear scan) anodic stripping voltammetry at mercury thin film hydrodynamic electrodes for reversible systems are examined, focussing on rotating disc and wall-jet disc electrodes. Stripping under forced convection is compared to non-convective stripping. Whereas rotating disc electrodes give experimental convective stripping peaks as predicted by diffusion layer theory, lower, broader peaks are found at wall-jet disc electrodes except at very high flow rates. The reasons for this are discussed and analysed.

### **INTRODUCTION**

The use of anodic stripping voltammetry (ASV) for the determination of a number of important trace metals at mercury thin film electrodes (MTFE) is now well established [1, 2]. It enables combination of the advantages of mercury as an electrode material, principally extended negative potential range, with forced convection during the deposition (preconcentration) step, resulting, in many cases, in enhanced sensitivity, resolution and reproducibility in relation to the hanging mercury drop electrode [3]. The mercury thin film, usually electrodeposited on a glassy carbon substrate, is either preformed prior to reducing the metal ions of interest on the surface of the film, or mercury is co-deposited with the metal (in situ mercury deposition [4]).

Following preconcentration, the stripping or redissolution step is carried out by linear potential scan, a pulse technique or (at hydrodynamic electrodes only) by collection of the stripped species at a second, downstream electrode such as the ring of a ring-disc electrode [5]. Whereas a linear potential scan gives a non-horizontal baseline due to capacitive contributions, the pulse and collection techniques both include discrimination against capacitive currents, enabling lower detection limits.

However, effective background subtraction enables the use of linear scan stripping (dcASV).

The use of forced convection during the stripping step [3,6–9] has not been widespread. It has been the general belief that convection causes an increase in noise, and that background subtraction is more difficult. With recent developments in hydrodynamic electrodes [10], this type of difficulty can be largely overcome. Widening interest in the use of hydrodynamic electrode detectors in a flow-through configuration [11], such as wall-jet or tubular/channel with their inherent advantages of good reproducibility, fast matrix exchange and use on-line, suggests an increasing use of forced convection throughout the entire ASV experiment.

The shape and position of dcASV stripping curves in a reversible system for stripping in stationary conditions was studied by de Vries and van Dalen [12] particularly considering the limit of mercury film thickness tending to zero, which corresponds to zero concentration gradient within the mercury film (zero concentration of oxidised species in bulk aqueous solution is assumed during redissolution). Experiment agrees well with theory [13]. As the film thickness tends to zero, the peak current  $i_p$ , peak half-width  $b_{1/2}$  and peak potential  $E_p$  relative to the half-wave potential  $E_{1/2}$ , are given by

$$i_p = 0.2975nFA\sigma c_R l \quad (1)$$

$$nb_{1/2} = 75.53 \text{ mV} \quad (2)$$

$$n(E_p - E_{1/2}) = -1.43 + 29.58 \log(l^2\sigma/D_R) \text{ mV} \quad (3)$$

where  $\sigma = (nF/RT)v$ ,  $l$  is the mercury film thickness,  $c_R$  the concentration of metal in the mercury film and  $D_R$  its diffusion coefficient. Peak current is directly proportional to scan rate, although as scan rate and/or mercury film thickness increase and transport within the film begins to play a part, the dependence tends to the square root of the scan rate, as predicted by the Sevcik–Randles relation [14].

The whole current peak may be expressed in terms of the formula

$$i = Z(\sigma t)nFA\sigma c_R l \quad (4)$$

where the current function  $Z(\sigma t)$  is a function of potential relative to  $E_p$ . When  $i = i_p$ ,  $Z(\sigma t) = 0.2975$  and we obtain eqn. (1). De Vries and van Dalen [12] presented values of  $Z(\sigma t)$  graphically; subsequently Stojek and Kublik [13] gave numerical values as a function of potential.

Roe and Toni [6] solved the time dependent convective diffusion equation for convective stripping at hydrodynamic MTFEs by using the diffusion layer concept and considering reversible systems; concentration gradients within the mercury film were ignored, corresponding to zero film thickness. They found reasonable agreement with experiment at rotating electrodes, as did other workers at rotating disc electrodes [3, 8] in terms of peak current and peak half-width. The expressions obtained are

$$i_p = 0.368nFA\sigma c_R l \quad (5)$$

$$n(E_p - E^{\circ'}) = 59.12 \log(\delta l\sigma/D_O) \text{ mV} \quad (6)$$

where  $D_O$  is the diffusion coefficient of the metal ion in aqueous solution. Once again the current peak may be expressed by the equation

$$i = Z(\sigma t) nFA\sigma c_R l \quad (4)$$

where  $Z(\sigma t)$  is given by

$$Z(\sigma t) = H - p \exp(-p) [\exp H + HEi(p) - HEi(H)] \quad (7)$$

Here,  $Ei$  is the exponential integral function, which is tabulated [15],  $p$  is a dimensionless parameter ( $= \text{const.} \times \exp(\sigma t)$ ), and  $H = (D_O c_O^\infty) / (\delta l \sigma c_R)$ , with  $c_O^\infty$  the concentration of metal ion in bulk solution. Under constant forced convection conditions in the deposition and stripping steps,  $H = (\sigma t_{\text{dep}})^{-1}$ . If  $H$  is sufficiently small (high enough scan rate or deposition time) then we get

$$Z(\sigma t) = p \exp(-p) \quad (8)$$

Bakanov et al. [7] considered the rotating disc MTFE under a variety of kinetic conditions.

Recently convective stripping dcASV at the wall-jet disc electrode has been studied experimentally [9] and, surprisingly, reasonable agreement found in the conditions employed with the theoretical response for non-convective stripping.

In this paper we reexamine the shape of dcASV curves at wall-jet and rotating hydrodynamic electrodes and their position on the potential axis for reversible systems.

## THEORY

### *Peak shape for convective and non-convective stripping*

To compare shapes of stripping curves under convective and non-convective stripping, we tabulate  $Z(\sigma t)$ . For convective stripping, consideration of eqns. (7) or (8) shows that  $i = i_p$  when  $p = 1$ . Since  $p = \text{const.} \times \exp(\sigma t)$  we can see that

$$(2.3RT/nF) \log p = \text{another constant} + n(E - E_p) \quad (9)$$

From this we can plot  $Z(\sigma t)$  as a function of potential.

Values of the current function at stationary and at hydrodynamic electrodes are shown in Table 1 as a function of  $n(E - E_p)$  and are presented graphically in Fig. 1.

As is clear from eqn. (4), since the peak area must remain constant, on going from non-convective to convective stripping, an increase in peak current is accompanied by a decrease in peak width. Convection depletes the mercury layer of metal more rapidly than by diffusion alone, giving the marked asymmetry in the hydrodynamic electrode peaks. This is reflected in the potentials at half peak height in Table 2. Asymmetry can be important for the resolution of adjacent current peaks.

The expression for the peak potential at hydrodynamic electrodes contains  $l$  explicitly. Nevertheless, if we remember that, for mercury deposition under diffusion limited current conditions

$$i_L = nFADc_{\text{Hg}}\delta_{\text{dep}} \quad (10)$$

TABLE 1

Values of current function  $Z(\sigma t)$ 

$n(E - E_p)/mV$	Convective stripping <sup>a</sup>	Non-convective stripping <sup>b</sup>
-150	0.0029	0.0026
-120	0.0092	0.0087
-110	0.0136	0.0128
-100	0.0199	0.0187
-90	0.0291	0.0233
-80	0.0424	0.0396
-70	0.0613	0.0571
-60	0.0877	0.0807
-50	0.1236	0.1123
-40	0.1705	0.1520
-30	0.2277	0.1982
-20	0.2900	0.2351
-15	0.3192	0.2658
-10	0.3441	0.2825
-5	0.3614	0.2935
-2.5	0.3662	0.2965
0	0.36788	0.29746
2.5	0.3661	0.2965
5	0.3605	0.2933
10	0.3373	0.2810
15	0.2983	0.2613
20	0.2465	0.2358
30	0.1288	0.1767
40	0.0411	0.1209
50	0.0063	0.0799
60	0.0003	0.0488
70	-	0.0302
80	-	0.0187
90	-	0.0117
100	-	0.0073
110	-	0.0046
120	-	0.0030
150	-	0.0008

<sup>a</sup> Using eqn. (8), this work.<sup>b</sup> Taken from ref. 13.

then for the conditions of a given experiment

$$l = \text{const.} \times \delta_{\text{dep}}^{-1} \quad (11)$$

Inserting this into eqn. (6) for convective stripping

$$n(E_p - E^{\circ'}) = \text{const.} + 59.12 \log(\delta\sigma/\delta_{\text{dep}}) \quad (12)$$

For any hydrodynamic electrode, uniformly or non-uniformly accessible, the peak

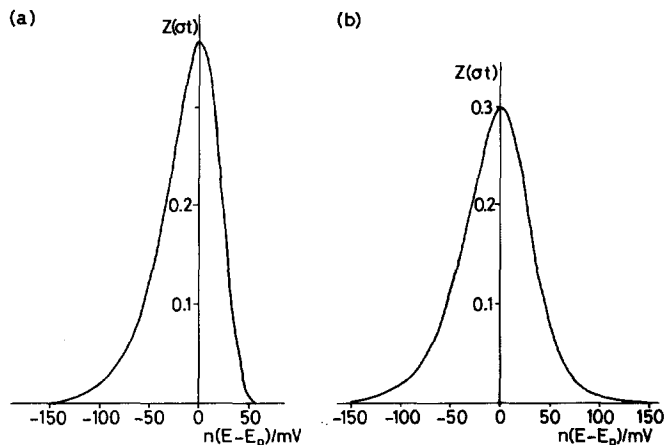


Fig. 1. Plots of current function  $Z(\sigma t)$  for linear scan stripping as a function of potential vs. peak potential: (a) convective (eqn. 8) and (b) non-convective [12, 13].

potential should be invariant over the electrode surface, since the ratio  $(\delta/\delta_{\text{dep}})$  will always be constant; the shape should also always be the same.

*Relation of peak shape under forced convection to linear sweep voltammetry of adsorbed reactants*

The approximation of zero mercury thin film thickness means that eqn. (4) is better written as

$$i = Z(\sigma t)nFA\sigma\Gamma_R \quad (13)$$

where  $\Gamma_R$  is the surface concentration of deposited species, reflecting the fact that in effect we should be considering the deposition step as normal electrodeposition onto a solid electrode. This suggests, for the limit of film thickness tending to zero, that stripping peaks can be compared directly with linear sweep voltammetry of irreversibly adsorbed reactants in stationary solution, since in each case only one rate

TABLE 2

Redissolution peak widths: differences between peak potentials and potentials at half peak height

	$n E_p - E_{p/2} /\text{mV}$		$nb_{1/2}/\text{mV}$
	Ascending portion	Descending portion	
Stationary	40.8	34.7	75.5
Hydrodynamic			
eqn. (8) ( $H = 0$ )	37.6	25.2	62.8
eqn. (7) ( $H = 10^{-2}$ )	36.1	25.8	61.9

limiting process is involved. Previously comparison has been made between equations for thin mercury films and those for thin layer cells [16].

The relevant equations are [17]

$$i = nFAk' \Gamma_R \exp[-(k'/(1-\alpha)\sigma)] \quad (14)$$

which can be rewritten as

$$i = Z(\sigma t) nFA\sigma \Gamma_R \quad (13)$$

with

$$Z(\sigma t) = (k'/\sigma) \exp[-(k'/(1-\alpha)\sigma)] \quad (15)$$

and  $k'$  the potential dependent redissolution rate constant. The peak potential is given by

$$n(E_p - E^{\circ'}) = (RT/(1-\alpha)nF) \ln((1-\alpha)\sigma/k') \quad (16)$$

For our case of the reversible convective stripping of adsorbed metal the rate is governed by diffusion in the diffusion layer, described by the mass-transfer coefficient  $k_0$ ; the charge transfer coefficient,  $\alpha$ , is put equal to zero in eqn. (15), leading to

$$i_p = 0.368nFA\sigma \Gamma_R \quad (17)$$

The same form of the equations compared to eqns. (4)–(6) is clear.

#### *Peak position: convective vs. non-convective stripping*

Inspection of eqns. (3) and (6) shows that under normal conditions, the peak potential will lie negative of  $E_{1/2}$  or  $E^{\circ'}$ .

Subtraction of eqn. (3) from eqn. (6) will give the relative positions of peaks for convective vs. non-convective stripping,  $\Delta E_p$ . In order to do this, we express  $E_p$  in eqn. (3) with respect to  $E^{\circ'}$ , using

$$E_{1/2} = E^{\circ'} + (RT/nF) \ln(D_R/D_O)^{1/2} \quad (18)$$

Since neutral species have relatively high diffusion coefficients in mercury ( $\approx 2 \times 10^{-5} \text{ cm}^2 \text{ s}^{-1}$ ) as compared to ions in aqueous electrolyte ( $\approx 6 \times 10^{-6} \text{ cm}^2 \text{ s}^{-1}$ ), the difference in  $E_{1/2}$  and  $E^{\circ'}$  is significant since in this case  $D_R \approx 3D_O$ . Substitution into eqn. (3) leads to

$$n(E_p - E^{\circ'}) = -1.43 + 29.58 \ln(l^2\sigma/D_O) \quad (19)$$

The difference in peak potential,  $\Delta E_p$ , is thus

$$\Delta E_p = (1/n) \{ 1.43 + 59.1 [\log \delta + \log \sigma^{1/2} - \log D_O^{1/2}] \} \quad (20)$$

This expression shows, as expected, that  $E_p$  becomes more positive with decrease in convection rate, increase in scan rate and decrease in  $D_O$ .

We present a representative example at each of rotating disc and wall-jet electrodes. The conditions considered are that  $n = 2$ ,  $D_O = 6 \times 10^{-6} \text{ cm}^2 \text{ s}^{-1}$ ,  $\nu = 9 \times 10^{-3} \text{ cm}^2 \text{ s}^{-1}$  and  $v = 10 \text{ mV s}^{-1}$ .

*Rotating disc electrode.* The diffusion layer thickness is given by [10]

$$\delta = 0.642 D_O^{1/3} \nu^{1/6} W^{-1/2} \quad (21)$$

If we take  $W = 4$  Hz, then  $\delta \approx 3 \times 10^{-3}$  cm and we obtain  $\Delta E_p \approx -30$  mV.

*Wall-jet disc electrode.* Unlike the rotating disc electrode, the wall-jet electrode is not uniformly accessible, the diffusion layer thickness being proportional to  $r^{5/4}$  [18] and given by

$$\delta = 6.12 D_O^{1/3} a^{1/2} \nu^{5/12} V_f^{-3/4} r^{5/4} \quad (22)$$

Assuming constant solution flow during the whole experiment, the redissolution peak potential should be constant over the electrode surface (eqn. 16). For typical values  $V_f = 0.03$  cm<sup>3</sup> s<sup>-1</sup>,  $r_1 = 0.15$  cm and an average diffusion layer thickness  $\bar{\delta} = (4/9)\delta(r_1)$ , we obtain  $\Delta E_p \approx -30$  mV once more.

If, however, the stripping step is carried out under purely diffusive conditions, then, since  $l$  varies over the electrode surface, eqn. (1) predicts that the corresponding value of  $E_p$  should also vary, resulting in a lowering of the peak current, peak broadening and increased asymmetry relative to a uniformly accessible electrode.

## EXPERIMENTAL

Experiments to test the predictions presented above, particularly those at the wall-jet disc electrode, were performed at a glassy carbon rotating disc electrode (radius 0.350 cm) and at a glassy carbon wall-jet disc electrode (radius 0.161 cm) with preformed thin mercury films. Electrodes were polished with 1  $\mu$ m diamond paste prior to use. Cell design is described elsewhere [11].

Solutions were prepared from Merck pro analysi reagents. Supporting electrolyte was 0.1 M KNO<sub>3</sub> + 0.005 M HNO<sub>3</sub> to which was added (i)  $2.0 \times 10^{-4}$  M Hg(II) for the mercury plating solution and (ii)  $1.0 \times 10^{-5}$  M Pb(II) for the ASV experiments. Solutions were deoxygenated with U grade ultra-pure oxyfree nitrogen for 15 min prior to and during experiments.

In rotating disc electrode (RDE) experiments the solution was changed by physically changing cells. The rotating assembly (Oxford Electrodes) gave rotation speed directly.

For the wall-jet experiments, gravity feed was used to bring the solution to the wall-jet disc electrode (WJDE). Flow rate was altered by changing the height of the solution reservoir and was measured volumetrically at frequent intervals. The solution reaching the wall-jet electrode was changed via a two-way tap placed before the cell.

The procedure involved plating mercury onto the glassy carbon electrode at  $-1.0$  V vs. SCE (RDE) or vs. Ag|AgCl (WJDE) for 600 s, and then changing the solution to that containing Pb(II). Lead deposition was carried out at  $-1.0$  V and the potential scanned in a positive direction at a predetermined scan rate with the sample solution continuing to flow. Deposition was assumed to continue during the stripping scan until the beginning of the redissolution peak, an approximation

found to work well. Further experiments with Pb(II) were carried out immediately or after removal (electrochemically or by wiping with a soft tissue) of the mercury film and formation of a new film, the effect of this being noted.

Potentials were controlled with a PAR 174A potentiostat and currents registered on a Houston RE0074 X-Y recorder.

## RESULTS AND DISCUSSION

### *Rotating disc electrode*

The applicability of the convective stripping relations for reversible systems at rotating disc electrodes, in terms of  $i_p$  and  $nb_{1/2}$  has been shown in previous studies [3,7,8] so long as there is a sufficiently thin mercury film, low enough scan rate, and high enough rotation speed. If these conditions are not satisfied, peaks are not as high and broader. As a general rule, scan rates between 2 and 50  $\text{mV s}^{-1}$  should suffice, although the upper limit increases with increasing rotation speed. Figure 2 shows an example of a lead redissolution wave: the agreement between theory and experiment is very good. Previous work has not concentrated on the shape of the full wave; however, we found good agreement under a wide variety of conditions. Deviations at potentials more negative than  $-100 \text{ mV}$  vs.  $E_p$  are probably due to difficulties in subtracting the sloping background current correctly.

Peak position follows eqn. (6) to a good approximation: doubling the value of the parameters in eqn. (6) should cause a movement of 9 mV, whereas it is in fact around 7 mV in all cases. This probably reflects the approximations in the

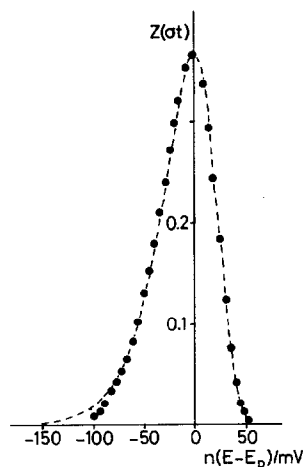


Fig. 2. Normalised current function for experimental stripping of Pb at rotating disc mercury thin film electrode (●) from preplated mercury film (600 s at  $W = 4 \text{ Hz}$ ;  $2 \times 10^{-4} \text{ M Hg}^{2+}$ ) and corresponding theoretical curve (---). Experimental conditions:  $W = 9 \text{ Hz}$ ,  $t_{\text{dep}} = 130 \text{ s}$ ,  $v = 2 \text{ mV s}^{-1}$ ,  $1.0 \times 10^{-5} \text{ M Pb}^{2+}$ .  $2b_{1/2} (\text{exptl}) = 63.0 \text{ mV}$ .



theoretical model. Comparison with stripping in stationary solution gives peak positions as expected. For example, under the conditions of the example in the theoretical section  $E_p$  (convective) =  $-0.490$  V vs. SCE whereas  $E_p$  (non-convective) =  $-0.462$  V.

#### Wall-jet disc electrode

Despite the non-uniform accessibility of the WJDE the Roe and Toni model [6] should be applicable as long as its assumptions can be satisfied. Previous work [9] affirmed that it is not, and comparison was made with the de Vries and van Dalen model [12] for stripping in stationary solution, although the justification for this is not clear.

In analysing the redissolution peaks it must be borne in mind that the area under the normalised current-voltage (i.e. current-time) redissolution curve must always be constant and equal to the charge passed during the preconcentration step. Figure 3 shows two typical area-normalised current-voltage profiles obtained at the WJDE at widely different flow rates in terms of the current function  $Z(\sigma t)$ . The profile at very high flow rate (Fig. 3a) is close to that expected for convective stripping; at the lower flow rate (Fig. 3b) the peak is broader and not as high. In the latter case, although the peak width at half-height ( $73.0/n$  mV) is reasonably similar to that of the stripping curve in stationary solution ( $75.5/n$  mV), the asymmetry expected for a hydrodynamic electrode is clear.

The peak half-widths of Table 3, some of which are considerably larger than for non-convective stripping from a uniformly accessible electrode ( $75.5/n$  mV), vary

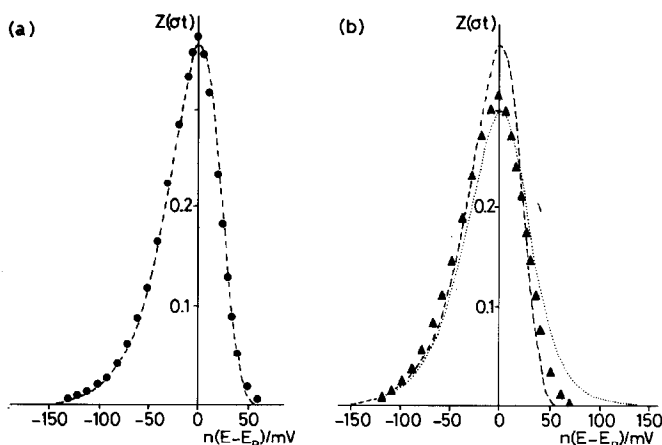


Fig. 3. Normalised current function for experimental stripping of Pb at wall-jet disc mercury thin film electrode from preplated mercury film (600 s at  $V_f = 0.053$  cm<sup>3</sup> s<sup>-1</sup>;  $2 \times 10^{-4}$  M Hg<sup>2+</sup>) and corresponding theoretical curves: (---) convective and (.....) non-convective. (a) (●) Experimental points.  $2b_{1/2} = 62.5$  mV. Experimental conditions:  $1.0 \times 10^{-5}$  M Pb<sup>2+</sup>,  $V_f = 0.154$  cm<sup>3</sup> s<sup>-1</sup>,  $t_{\text{dep}} = 47$  s,  $v = 5$  mV s<sup>-1</sup>; (b) (▲) Experimental points.  $2b_{1/2} = 73.0$  mV. Experimental conditions:  $1.0 \times 10^{-5}$  M Pb<sup>2+</sup>,  $V_f = 0.069$  cm<sup>3</sup> s<sup>-1</sup>,  $t_{\text{dep}} = 50$  s,  $v = 2$  mV s<sup>-1</sup>.

TABLE 3

Experimental peak half-widths at WJDE as function of volume flow rate and of scan rate for redissolution of Pb ( $n = 2$ )<sup>a</sup>

$V_f/\text{cm}^3 \text{ s}^{-1}$	$v/\text{mV s}^{-1}$	$2b_{1/2}/\text{mV}$	$V_f/\text{cm}^3 \text{ s}^{-1}$	$v/\text{mV s}^{-1}$	$2b_{1/2}/\text{mV}$
0.017	2	67.5	0.047	10	80.0
0.017	5	72.3	0.047	20	92.5
0.017	10	85.0	0.154	2	62.0
0.017	20	100.0	0.154	5	63.0
0.047	2	65.0	0.154	10	73.0
0.047	5	70.0	0.154	20	84.5

<sup>a</sup> For convective stripping  $nb_{1/2} = 62.8 \text{ mV}$ ; for non-convective  $nb_{1/2} = 75.5 \text{ mV}$  (see Table 2).

considerably, increasing with increasing scan rate and with decreasing flow rate. The explanation put forward in ref. 9 of following the non-convective stripping model cannot be correct. At the wall-jet electrode (or any other non-uniformly accessible electrode) we must consider, besides scan rate:

(a) differences in electrode kinetic regimes over the electrode surface owing to changes in the mass transfer coefficient  $k'_0$  ( $\propto \delta^{-1}$ ) since for a reversible system  $k'_0 \gg k'_D$  [19];

(b) diffusion parallel to the electrode surface within a relatively thick diffusion layer altering the concentration profile; clearly the larger  $k'_D$ , i.e. higher convection, the less this will be important.

Both (a) and (b) result in peak current lowering and increasing peak width, the effects becoming less important on increasing convection rate. These two factors are able to explain the experimental observations.

Peak potentials alter as predicted. For example for the conditions specified in the theoretical section, except for the volume flow rate ( $V_f = 0.047 \text{ cm}^3 \text{ s}^{-1}$ ) we calculate  $\Delta E_p \approx 35 \text{ mV}$ . Experimentally,  $E_p(\text{convective}) = -0.525 \text{ V}$  vs. Ag|AgCl and  $E_p(\text{stationary}) = -0.491 \text{ V}$ , so agreement is satisfactory.

#### *Mercury thin film history at the WJDE*

An effect of mercury thin film history is observed: the second and subsequent scans on a preformed mercury film invariably give rise to lower, broader peaks. Visual inspection of the electrode surface at this stage invariably shows a thinning of the mercury film in the exact centre of the disc where the jet impinges. It is generally accepted that a mercury film on glassy carbon consists of very tiny droplets [20], which could be subject to movement on the electrode surface: some of the mercury at the electrode centre possibly migrates radially or leaves the electrode surface. Whatever the reason, the effect will be to make the thickness of the mercury film more uniform.

#### *Uniformly thick mercury film at the WJDE*

We consider the limiting case of a uniformly thick film at a wall-jet disc electrode using the diffusion layer concept. In this case,  $\delta_{\text{dep}}$  is constant and so

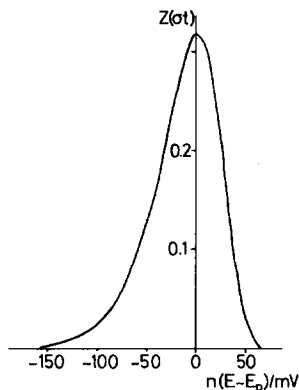


Fig. 4. Plot of current function  $Z(\sigma t)$  as a function of potential at wall-jet electrode for convective stripping from uniformly thick mercury film. Peak half-width =  $42.9/n + 30.9/n = 73.8/n$  mV.

$(\delta/\delta_{\text{dep}})$  varies over the electrode surface (eqn. 16). The effect that  $\delta$  has on the position of the curve on the potential axis is given by  $(59.1/n) \log \delta$ . Dividing the electrode into a central disc and  $(n - 1)$  concentric rings, all of equal width, then for each section we can calculate an approximate average diffusion layer thickness

$$\bar{\delta} = \text{const.} \times (r_i^{5/4} + r_o^{5/4})/2 \quad (23)$$

where  $r_o$  is the outer radius of the section,  $r_i$  its inner radius and  $\bar{\delta}$  the area weight. Summation of the various contributions to the final peak are calculated using eqn. (8). The resulting peak for large  $n$  ( $n = 50$  gives  $< 0.1\%$  error) is shown in Fig. 4. The current function at  $i = i_p$  has been reduced from 0.368 to 0.318, still 7% higher than the stationary electrode value of 0.297; peak width at half height is  $73.8/n$  mV.

It should be noted that, in principle, we should obtain the curve of Fig. 4 if we can deposit a uniform thin mercury film on a suitable electrode substrate. Dipping of copper in liquid mercury has been suggested as an alternative method to electrodeposition on glassy carbon for mercury thin film formation [21]. Advantages for the electrode centre where the jet impinges are clear; disadvantages could arise from the mercury film being too thick and difficulty of renewing the mercury film without removing the electrode from the cell.

## CONCLUSIONS

Convective stripping gives rise to narrower, higher and more asymmetric stripping peaks than in stationary solution, useful for peak resolution. Although, under commonly used convective conditions, the rotating disc electrode gives rise to narrower peaks than the wall-jet electrode, the latter, as a flow detector, does not suffer from any problems of depletion and offers significant practical advantages in sample throughput and use on-line.

The shape of the stripping peaks on increasing the convection rate changes significantly at the wall-jet disc electrode and to a small extent at the rotating disc electrode.

Even when, at the wall-jet, peaks are broader than predicted, their asymmetry can still be useful in peak resolution. Codeposition of mercury with the metal ion of interest reduces problems of mercury movement in the impingement zone, and tends to lead to improved reproducibility.

Finally, problems of large concentrations of oxidised species appearing close to the electrode surface in aqueous solution are avoided.

#### GLOSSARY OF SYMBOLS

$a$	Diameter of jet in wall-jet electrode
$A$	Electrode area
$b_{1/2}$	Peak width at half-height
$c_{\text{Hg}}$	Concentration of Hg(II) in solution during mercury electrodeposition
$c_{\text{O}}^{\infty}$	Concentration of metal ion in bulk aqueous solution
$c_{\text{R}}$	Concentration of metal in mercury film before stripping begins
$D_{\text{O}}$	Diffusion coefficient of metal ion in aqueous solution
$D_{\text{R}}$	Diffusion coefficient of metal in mercury layer
$E^{\circ'}$	Formal electrode potential
$E_{1/2}$	Half-wave potential
$E_{\text{p}}$	Peak potential of stripping curve
$\Delta E_{\text{p}}$	Difference between peak potentials with and without forced convection
$H$	See eqn. (7) ( $= (\sigma t_{\text{dep}})^{-1}$ )
$i_{\text{L}}$	Diffusion limited current at hydrodynamic electrode
$i_{\text{p}}$	Peak current (at $E_{\text{p}}$ )
$k'$	Rate constant for redissolution of adsorbed reactants
$k'_0$	Standard rate constant for electrode reaction
$k'_{\text{D}}$	Mass transfer coefficient
$l$	Thickness of mercury film
$n$	Number of electrons transferred
$p$	Dimensionless parameter in eqns. (7) and (8)
$r_1$	Radius of disc electrode
$r_i$	Inner radius of section of disc electrode
$r_o$	Outer radius of section of disc electrode
$t_{\text{dep}}$	Deposition time
$v$	Scan rate
$V_{\text{f}}$	Volume flow rate
$W$	Rotation speed of rotating electrode (in Hz)
$Z(\sigma t)$	Current function describing stripping peak (eqn. 4)
$\alpha$	Transfer coefficient
$\Gamma_{\text{R}}$	Surface concentration of adsorbed reduced species
$\delta$	Diffusion layer thickness at hydrodynamic electrode

$\delta_{\text{dep}}$	Diffusion layer thickness at hydrodynamic electrode during deposition
$\nu$	Kinematic viscosity of aqueous solution
$\sigma$	Function of scan rate ( $= (nF/RT)v$ )

## REFERENCES

- 1 Kh.Z. Brainina, *Stripping Voltammetry in Chemical Analysis*, Halsted Press, New York, 1974.
- 2 J. Wang, *Stripping Analysis. Principles. Instrumentation and Applications*, VCH Publishers, Deerfield Beach, FL, 1985.
- 3 G.E. Batley and T.M. Florence, *J. Electroanal. Chem.*, 55 (1974) 23.
- 4 T.M. Florence, *J. Electroanal. Chem.*, 27 (1970) 273.
- 5 J. Wang, ref. 2, pp. 22–42.
- 6 D.K. Roe and J.E.A. Toni, *Anal. Chem.*, 37 (1965) 1503.
- 7 V.I. Bakanov, M.S. Zakharov, V.A. Antip'eva and A.P. Grigorchenko, *Zh. Anal. Khim.*, 28 (1973) 2292.
- 8 V.I. Bakanov, M.S. Zakharov, V.A. Antip'eva and A.P. Grigorchenko, *Zh. Anal. Khim.*, 29 (1974) 421.
- 9 H. Gunasingham, K.P. Ang and C.C. Ngo, *J. Electroanal. Chem.*, 215 (1986) 123.
- 10 C.M.A. Brett and A.M. Oliveira Brett in C.H. Bamford and R.G. Compton (Eds.), *Comprehensive Chemical Kinetics*, Vol. 26, Elsevier, Amsterdam, 1986, Ch. 5.
- 11 K. Stulik and V. Pacakova, *Electroanalytical Measurements in Flowing Liquids*, Ellis Horwood, Chichester, 1987.
- 12 W.T. de Vries and E. van Dalen, *J. Electroanal. Chem.*, 14 (1967) 315.
- 13 Z. Stojek and Z. Kublik, *J. Electroanal. Chem.*, 105 (1979) 247.
- 14 J.E.B. Randles, *Trans. Faraday Soc.*, 44 (1948) 327; A. Sevcik, *Collect. Czech. Chem. Commun.*, 13 (1948) 349.
- 15 M. Abramowitz and I.A. Stegun, *Handbook of Mathematical Functions*, Dover, New York, 1965, pp. 238–243.
- 16 A.J. Bard and L.R. Faulkner, *Electrochemical Methods: Fundamentals and Applications*, Wiley, New York, 1980, p. 413.
- 17 E. Laviron, *J. Electroanal. Chem.*, 52 (1974) 355.
- 18 W.J. Albery and C.M.A. Brett, *J. Electroanal. Chem.*, 148 (1983) 201.
- 19 W.J. Albery, *Electrode Kinetics*, Clarendon Press, Oxford, 1975, p. 63.
- 20 M. Stulikova, *J. Electroanal. Chem.*, 48 (1973) 33.
- 21 P.J. Daly, D.J. Page and R.G. Compton, *Anal. Chem.*, 55 (1983) 1191.